ACS APPLIED MATERIALS & INTERFACES

Research Article

www.acsami.org

Influence of Film Thickness and Oxygen Partial Pressure on Cation-Defect-Induced Intrinsic Ferromagnetic Behavior in Luminescent p-Type Na-Doped ZnO Thin Films

S. Ghosh,*[,†] Gobinda Gopal Khan,[†,†] Shikha Varma,[§] and K. Mandal[†]

[†]Department of Condensed Matter Physics and Material Sciences, S. N. Bose National Centre for Basic Sciences, Salt Lake City, Kolkata 700 098, India

[§]Institute of Physics, Bhubaneswar 751005, India.

ABSTRACT: In this article, we have investigated the effect of oxygen partial pressure (P_{O_2}) and film thickness on defect-induced room-temperature (RT) ferromagnetism (FM) of highly c-axis orientated p-type Na-doped ZnO thin films fabricated by pulse laser deposition (PLD) technique. We have found that the substitution of Na at Zn site (Na_{Zn}) can be effective to stabilize intrinsic ferromagnetic (FM) ordering in ZnO thin films with Curie temperature (T_C) as high as 509 K. The saturation magnetization (M_S) is found to decrease gradually with the increase in thickness of the films, whereas an increase in "M_S" is observed with the increase in P_{O_2} of the PLD chamber. The enhancement of ferromagnetic signature with increasing P_{O_2} excludes the possibility of oxygen vacancy (V_O) defects for the magnetic origin in Na-doped ZnO films. On the other hand, remarkable enhancement in the green emission (I_G) are observed in the photoluminescence (PL) spectroscopic measurements due to Na-doping and that indicates the stabilization of considerable amount of Zn vacancy (V_{Zn})-type defects in Na-doped ZnO films. Correlating the results of PL and X-ray photoelectron spectroscopy (XPS) studies with magnetic measurements we have found that V_{Zn} and Na substitutional (Na_{Zn}) defects are responsible for the hole-mediated FM in Na-doped ZnO films, which might be an effective candidate for modern spintronic technology.

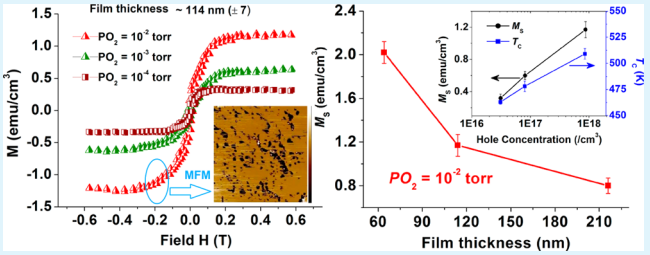

KEYWORDS: *zinc oxide, Na substitution, zinc vacancy, ferromagnetism, photoluminescence*

1. INTRODUCTION

Zinc oxide, which an important n-type wide band-gap (~3.3 eV) semiconductor can provide an exciting possibility of merging electronics, photonics, and magnetics for the application to new spin-based multi-functional devices. In this regard, investigation of defect-induced room-temperature (RT) ferromagnetism (FM) in ZnO-based semiconductor has been drawn immense attention to the scientists as an alternative approach to prepare new class of dilute magnetic semiconductors (DMS)[1,2] for modern spintronic and opto-spintronic technology.[3,4] The observation of unexpected RT FM in pure HfO_2 thin film[5] has opened up a new challenge to explain the origin of magnetic moment without the presence of any d or f-orbital electrons. After that the experimental evidence of RTFM were also observed in case of different oxide thin films and nanostructures such as ZnO, SnO_2, TiO_2, In_2O_3, etc., in their purest phase[6−10] or even using dopant elements that are completely nonmagnetic.[11−14] The theoretical calculations performed in case of different oxides such as HfO_2,[15] CaO,[16] SnO_2,[17] and ZnO[18] revealed that cation vacancies can induce a magnetic moment, which is found to be localized at the vacancy site, and the ferromagnetic ordering between these cation vacancies is energetically favorable when vacancy concentration reaches above a threshold concentration. Sundaresan et al.[6] have reported that FM is a universal property of oxide nanostructures where they have attributed oxygen vacancy (V_O) defects for the origin of observed FM. However, density functional theory (DFT)-based first principle investigation have shown that neutral V_O is non-magnetic whereas Zn and Sn vacancy in ZnO and SnO_2 matrix, respectively, can have magnetic moment originating from the unpaired 2p orbital of O atom in the vicinity of cation vacancy site.[17,18]

However, the stabilization and proper control of cation vacancy-type defects are found to be very difficult due to their high formation energy. Bouzerar et al.[19] have suggested in case of HfO_2 or ZrO_2 that the stabilization of high-temperature FM could be easier through the cationic substitution of the nonmagnetic elements like Li, Na, K, Rb, or Cs rather than Hf or Zr vacancy. Recently Yi et al.[12] have reported that the formation energy of V_{Zn} in ZnO can be reduced substantially by Li substitution (Li_{Zn}) at Zn site and the magnetic moments of both V_{Zn} and Li_{Zn} defects are found to be mediated

Received: November 9, 2012
Accepted: March 5, 2013
Published: March 5, 2013

ferromagnetically in p-type ZnO films. In the case of Li or K-doped ZnO nanowires, in our previous report,[20,21] we also have shown the evidence of strong ferromagnetic interaction due to Li or K substitution and the co-doping of Li−N found to be even more effective than the Li-doping alone.[21] In all the cases, it is found that the V_{Zn} defects are playing a crucial role to stabilize RTFM in p-type ZnO. Wang et al.[18] have shown that the V_{Zn} always prefers to reside on the surface of the material and the magnetic moment of V_{Zn} defects lies the surface become larger compared to the V_{Zn} lies deep inside the bulk. Hence, it is always expected that such vacancy-induced FM in ZnO should depend explicitly on the dimension of the film such as film thickness. Furthermore, in order to build grip on such new class of RT-ferromagnetic ZnO-based DMS for practical application, it is very necessary to control the defect formation and also to parameterise such defects with respect to the various experimental conditions. Hence, in this work, we have investigated defect-induced magnetic properties of a series of Na-doped ZnO thin films with various film-thicknesses deposited under a specified level of oxygen partial pressure (P_{O_2}) of pulse laser deposition (PLD) chamber. At the same time, for fixed film-thickness, the Na-doped ZnO films are also deposited by changing the level of P_{O_2}. We have found that the defects mostly located at the cation site such as Zn vacancy (V_{Zn}) and substitutional Na (Na_{Zn}) defects are responsible for the RTFM in Na-doped ZnO films. Our study also indicates that the stabilization of such cation-defects-induced RTFM in Na-doped ZnO films is most favorable in the film with relatively low thickness (<70 nm) and prepared under high level of P_{O_2} (>1 × 10^{-2} Torr).

2. EXPERIMENTAL DETAILS

Pure and Na-doped ZnO thin films are deposited by pulse laser deposition (PLD) technique on the c-axis-sapphire (Al_2O_3) substrate using a KrF excimer laser of power density of 2.14 J/cm^2 and pulse repetition rate of 5 Hz. High purity ZnO and Na-acetate (99.99%) powders are mixed in appropriate ratio have been palletized and then sintered at 800° C to prepare of targets for 6 at.% Na-doped ZnO films. The base pressure of the deposition chamber and the substrate temperature was maintained at 5 ×10^{-5} Torr and 500° C, respectively. Keeping the PO_2 of the PLD chamber fixed at a particular level, the thickness of the $Zn_{0.94}Na_{0.06}O$ films is varied from 69 to 216 nm by changing the total numbers of laser shots. Another sets of $Zn_{0.94}Na_{0.06}O$ films with constant thickness are prepared by changing the level of PO_2 from 10^{-4} to 10^{-2} Torr. The crystallographic phases of the all the pure ZnO and $Zn_{0.94}Na_{0.06}O$ films were identified by x-ray diffraction (XRD, X'Pert Pro, Panalytical), while the magnetic measurements were performed by superconducting quantum interference devices (SQUID). Photoluminescence (PL) spectroscopic measurements were conducted to realise the defect-levels transitions between the optical band-gap of Na-doped thin films by using a spectrofluorometer (Horiba Jobin Yvon, Fluorolog-3) having Xe lamp source. The chemical composition of Na-doped ZnO films and the substitution of Na^{1+} ion at Zn site within the ZnO lattice were confirmed by X-ray photoelectron spectroscopy (XPS). Hall measurement was conducted to estimate the carrier concentrations and the types (n-type/p-type) of the semiconducting films.

3. RESULTS AND DISCUSSION

The crystallographic phases of pure ZnO and $Zn_{0.94}Na_{0.06}O$ films are indentified using grazing incidence XRD (GI-XRD), shown in Figure 1. The observation of only ZnO (002) and (004) diffraction peak indicates that the ZnO film have hexagonal wurtzite crystal structure and highly oriented along

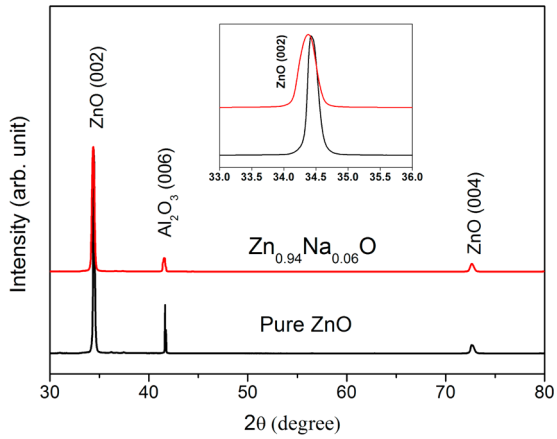

Figure 1. XRD pattern of pure ZnO and $Zn_{0.96}Na_{0.06}O$ thin films. Inset: High-magnification view of the ZnO (002) diffraction peak that indicates the shifting of (002) diffraction peak towards lower 2θ direction for Na-doped ZnO film.

the c-axis [001] direction. The preferential growth of ZnO thin films along the [001] direction are due to the fact that the ZnO films are deposited on (001) sapphire (c-plane Al_2O_3) substrates. As both ZnO and Al_2O_3 substrate has hexagonal crystal structure with definite c/a ratio, the ZnO film prefers to grow along the existing growth direction of the Al_2O_3 substrate which is [001] here. However, it is also noticeable that the intensity of the (006) diffraction peak of the thick c-Al_2O_3 substrate (~1 mm) is very weak compared with the diffraction peaks for very thin ZnO films (only 64-194 nm). It happens because here we have conducted the GI-XRD measurements. The GI-XRD technique uses small incident angle (~1° with the film surface) for the incoming X-ray beam, so that diffraction can be made only surface sensitive and thus it is quite able to avoid the strong diffraction peaks arising from the thicker substrate. In addition, the ZnO (002) peak for Na-doped ZnO film is found to be shifted towards lower 2θ direction (inset of Figure 1) which confirms the successful substitution of large Na^+ ions (radius ~0.097 nm) replacing smaller Zn^{2+} ions (radius ~0.074 nm).[22] The increase in the peak width of ZnO with Na-doping signifies a reduction of the crystallite size for Na-doped ZnO films. Hall measurement was performed to estimate the carrier concentrations and the types (n-type/p-type) of the semiconducting films. All the Na-doped ZnO films are found to be p-type while the pure ZnO film is found to be n-type. The substitution of monovalent Na at divalent Zn stie can introduce holes into the system and therefore, the transformation from n-type to p-type ZnO due to Na-doping is possible. Figure 2 shows the variation of carrier (hole) concentrations (η), film resistivity (ρ) and carrier mobility (μ) in case of the Na-doped ZnO films with similar thickness (~114 nm) grown at different oxygen partial pressures (P_{O_2} = 1 × 10^{-3}, 1 × 10^{-4}, and 1 × 10^{-2} Torr). The hole concentration is found to increase gradually with increase of PO_2, whereas the values of film resistivity and carrier mobility are found to decrease with PO_2.

Figure 3a shows the RT field-dependent magnetization (M-H) measurements for $Zn_{0.94}Na_{0.06}O$ films of different thicknesses prepared under PO_2 ~10^{-2} Torr. All the $Zn_{0.94}Na_{0.06}O$ films with various thicknesses are found to exhibit significant FM at RT. It is important to notice that the $Zn_{0.94}Na_{0.06}O$ film with lowest thickness (~ 64 nm) exhibits

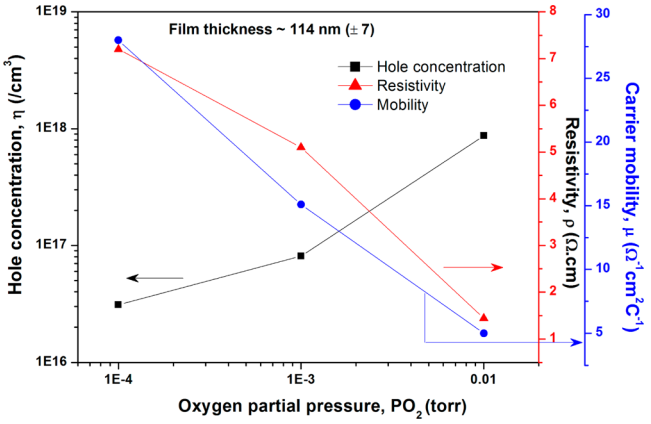

Figure 2. Variation in carrier (hole) concentration (η), film resistivity (ρ) and carrier mobility (μ) in case of the Na-doped ZnO films with similar thickness (~114 nm) grown at different oxygen partial pressures (P_{O_2} = 1 × 10^{-3}, 1 × 10^{-4}, and 1 × 10^{-2} Torr).

largest saturation magnetization (M_S) ~ 2.02 emu/cm^3 and the value of M_S decreases gradually with increasing film thickness. Figure 3b shows a representative temperature-dependent magnetization, $M(T)$ data for $Zn_{0.94}Na_{0.06}O$ film of 114 nm thick. The values of Curie temperatures (T_C) estimated from the high temperature M (T) measurements are found to be well above the RT (300 K). However, like M_S, the values of T_C are also found to decrease consistently with increasing of the film-thickness. The highest value of T_C (~526 K) obtained for 64 nm thick $Zn_{0.94}Na_{0.06}O$ film. RT ferromagnetic behaviour is also observed even in case of undoped ZnO film of ~69 nm thick, but the value of M_S is found to be one order less in magnitude compared to the $Zn_{0.94}Na_{0.06}O$ film with similar thickness (~64 nm) prepared under same level of P_{O_2} (~1 × 10^{-2}) Torr. However, the pure ZnO film with larger thickness (~196 nm) no RTFM is observed (not shown here), instead showed a diamagnetic behaviour. Therefore, the observation the RTFM in low thickness films indicates that significant change of structural defects which might be playing crucial role to stabilize magnetic interaction.

In order to visualize the domain structures and domain configuration inside the ferromagnetic films, magnetic force microscope (MFM) have been used. Images c and d in Figure 3 show the comparison of the MFM micrographs of pure ZnO (~69 nm thick) and $Zn_{0.94}Na_{0.06}O$ films (~64 nm thick), respectively. The existence of strong ferromagnetic ordering in $Zn_{0.94}Na_{0.06}O$ film can be visualize through the regular distribution of magnetic domains where the bright and dark contrasts correspond to high concentrations of positive and negative poles, respectively. On the other hand, the MFM micrograph of pure ZnO film with a few irregular, defused grains signifies its relatively weak ferromagnetic ordering. The dependency of ferromagnetic signature in $Zn_{0.94}Na_{0.06}O$ film on the oxygen partial pressure (P_{O_2}) under which the films were deposited, have also been examined and the corresponding M–H measurements are shown in Figure 4a. The film grown under highest level of "P_{O_2}" (~1 × 10^{-2} Torr) is found to exhibit largest $M_S \approx$ 1.17 emu/cm^3 and the values of M_S is found to decrease consistently with the decrease of P_{O_2} (inset of Figure 4a). This is quite interesting observation because the film

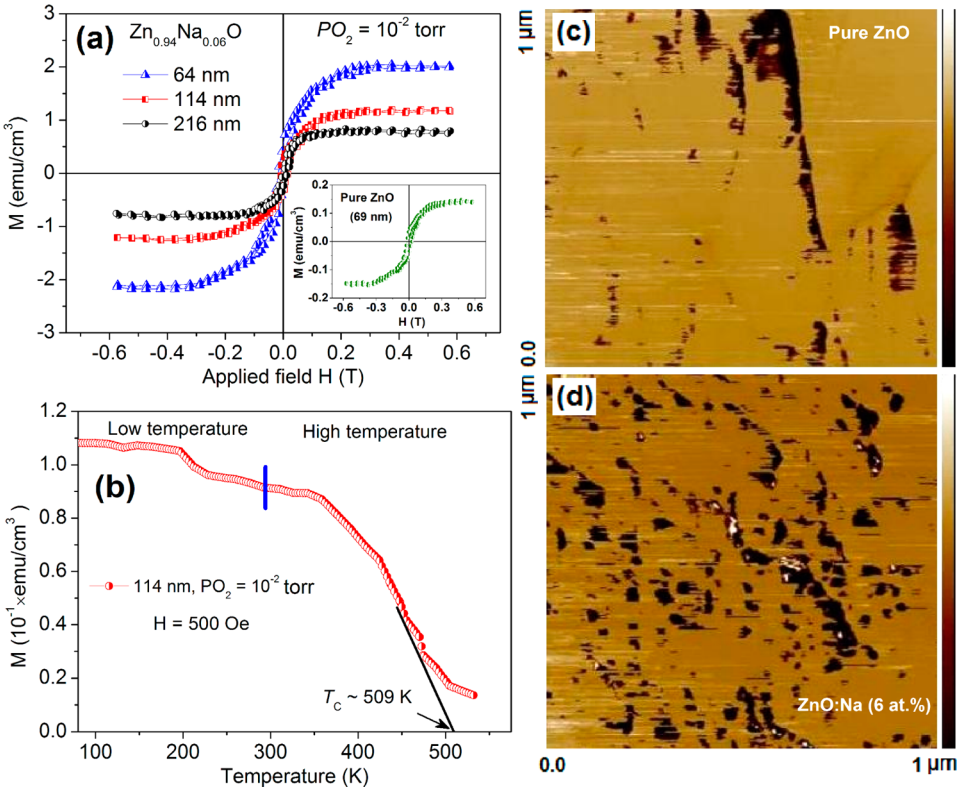

Figure 3. (a) Room-temperature M–H measurements for $Zn_{0.94}Na_{0.06}O$ films with various thicknesses prepared under P_{O_2} ~ 1 × 10^{-2} Torr. Inset: M–H behaviour of pure ZnO film at 300 K. (b) Temperature-dependent magnetization, $M(T)$ curves for 114 nm thick $Zn_{0.94}Na_{0.06}O$ film. MFM micrographs of (c) pure ZnO and (d) $Zn_{0.94}Na_{0.06}O$ film revealing the individual domain configurations within the films.

dx.doi.org/10.1021/am302649r | ACS Appl. Mater. Interfaces 2013, 5, 2455–2461

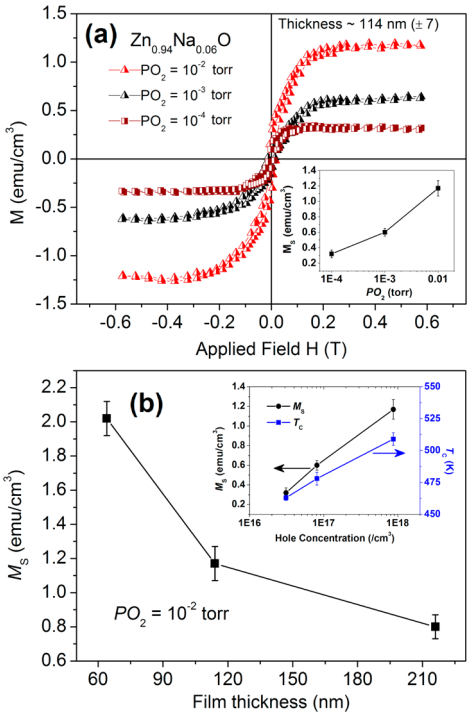

Figure 4. (a) Room-temperature $M-H$ measurements for similar thick (~ 114 nm) $Zn_{0.94}Na_{0.06}O$ films prepared under different levels of P_{O_2}. Inset: Change in M_S with the level of PO_2. (b) Variation of M_S of $Zn_{0.94}Na_{0.06}O$ films with the film-thickness, Inset: The change of M_S and T_C with the hole concentration (n) in the 114 nm thick $Zn_{0.94}Na_{0.06}O$ films grown at different oxygen partial pressure (PO_2= 1 × 10^{-2}, 1 × 10^{-3}, and 1 × 10^{-4} Torr).

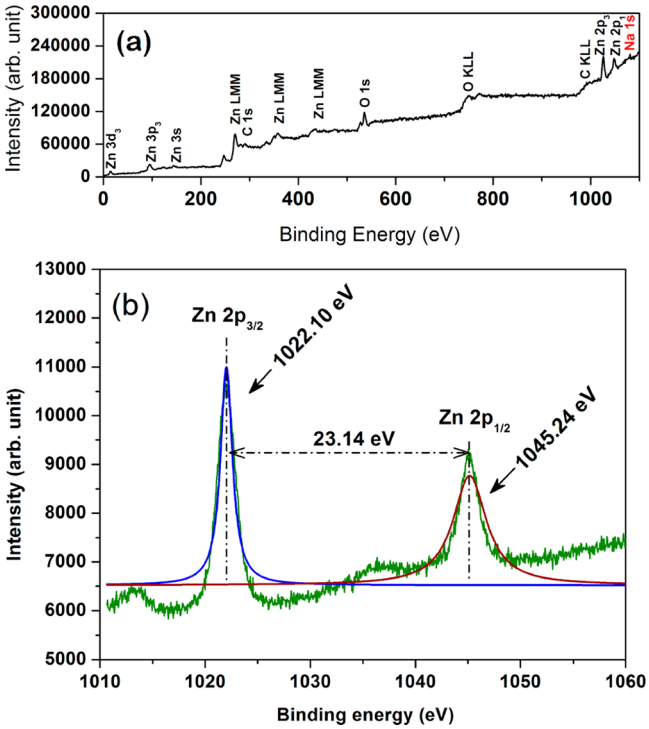

Figure 5. (a) Typical XPS survey scan of $Zn_{0.94}Na_{0.06}O$ film using Mg K_α source and (b) high resolution XPS spectra of (b) Zn 2p, core level in $Zn_{0.94}Na_{0.06}O$ film. (c) O 1s and (d) Na 1s core level.

prepared under low level of P_{O_2} should have contain more oxygen vacancy (V_O) defects.[23] Hence, if the magnetic moments were associated with the V_O defects then the film fabricated under low P_{O_2} should exhibit larger magnetic moment. On the contrary, the gradual decrease of M_S with lowering of PO_2 clearly indicates the magnetic moment in Na-doped ZnO films is not associated with V_O defects and must be originated from any other defects. The values of M_S and T_C of Na-doped ZnO films with similar thickness (~114 nm) are plotted against the corresponding hole concentration, as shown in the inset of Figure 4b. It is noticeable that both M_S and T_C in the $Zn_{0.94}Na_{0.06}O$ films (~114 nm) increase with the increase of hole concentration. This observation gives the indication of hole-mediated ferromagnetic interaction in Na-doped ZnO films. On the contrary, the FM observed in case of pure ZnO film seems to be electron-mediated as the undoped material is found to be n-type.

Figure 5 shows the XPS survey scan for $Zn_{0.94}Na_{0.06}O$ film using Mg K_α source and the high-resolution XPS spectra of Zn 2p core level. From the XPS scan, (Figure 5a), no impurity elements except carbon (C) are detected in within the detection limit of XPS. The C 1s (284.6 eV) peak is usually used as an internal reference in the spectrum.[24] The C 1s peak may also be because of the carbon tape used during the measurements. The core level Zn 2p spectrum (Figure 5b) displays a doublet located at 1022.10 and 1045.24 eV respectively corresponds to the core lines of Zn $2p_{3/2}$ and $2p_{1/2}$. The binding energy difference (23.14 eV) between the two peaks of the Zn 2p spectrum clearly indicates that the Zn is in the +2 oxidation state.[24,25] The core level of O 1s peak at 530.64 eV, shown in Figure 6a, indicates the Zn−O bond in the hexagonal wurtzite ZnO crystal structure,[26] whereas the observation Na 1s core level peak at 1071.40 eV (Figure 6b) confirms the presence of Na−O bond due to substitution of Na^{1+} at Zn^{2+} Site (Na_{Zn}) within ZnO lattice.[24,27−29] No evidence of metallic Na is observed in Na-doped ZnO films. Although it is also possible that some fraction (a little amount) of Na atoms may occupy the lattice interstitial site which can give rise to small shoulder peak at low binding energy than the substituted Na^{1+}. However, here, in the Na 1s spectra we have not observed such evidence. In addition, the evidence of substituted Na^{1+} at Zn site has been observed during analysis of X-ray diffraction patterns also. Therefore, we believe that the majority of Na atoms are substituted at Zn site (Na_{Zn}) within the ZnO lattice. The Na_{Zn} defect is known to create shallow acceptor states, which can be responsible for the p-type conductivity of the Na-doped ZnO films,[30,31] as observed from the Hall measurements. The Na-doping concentration within the ZnO is also estimated from XPS analysis and found to be consistent within the range of 5.66 to 5.84 at %, which is less than the nominal concentration of 6 at %.

Figure 7a shows the room-temperature PL spectra of the pure ZnO and $Zn_{0.94}Na_{0.06}O$ films of almost similar thickness prepared under various level of P_{O_2} under an excitation wavelength (λ_{ex}) of 330 nm. The PL spectrum of the pure and the Na-doped ZnO thin films is found to be exhibit both the defect-related and ultraviolet-visible (UV) emissions. With the incorporation of Na in ZnO, the UV (peak 1) emission is found to suppress considerably due to the dominance of defect-related emissions like green (peak 2, ~2.38 eV) and yellow-orange emission (peak 3, ~2.20 eV). It is found that both the UV and the defect related bands becomes broad and red shifted in the Na-doped ZnO films compared with that of the pure

dx.doi.org/10.1021/am302649r | ACS Appl. Mater. Interfaces 2013, 5, 2455−2461

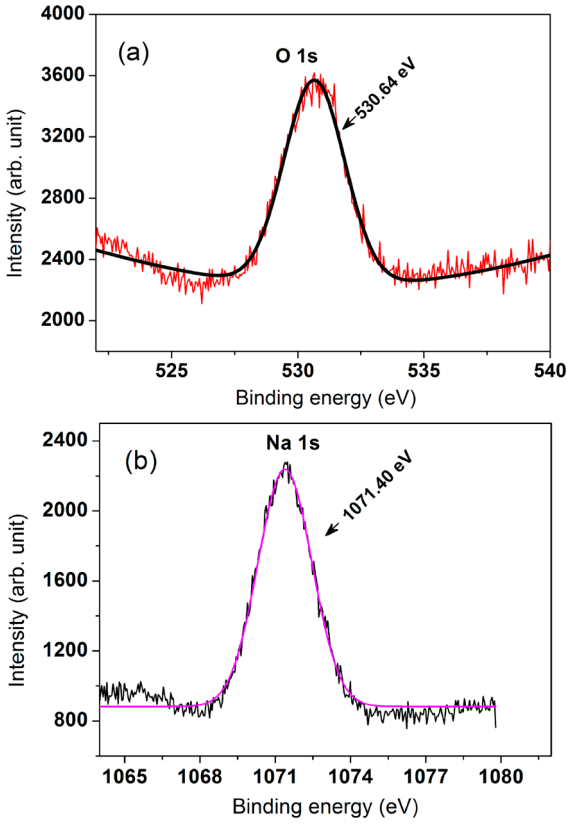

Figure 6. XPS spectra of (a) O 1s and (b) Na 1s core level in $Zn_{0.94}Na_{0.06}O$ film.

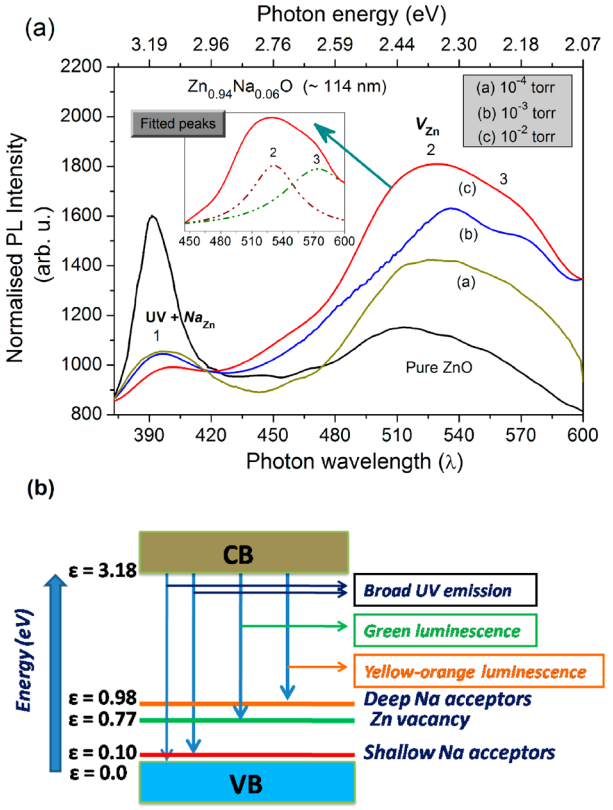

Figure 7. (a) Room-temperature PL spectra of similar thick (~114 nm) $Zn_{0.94}Na_{0.06}O$ films prepared under various level of P_{O_2}. (b) Schematic energy band diagram exposing the position of different defect states within the ZnO energy band gap and their electronic transitions occurring during PL emission.

ZnO film. The UV emission (peak 1) at 3.18 eV in the pure ZnO film is associated to the near band edge (NBE) emission due to the free exciton (FX) recombination through an exciton−exciton collision process.[32] The substitutional Na (Na_{Zn}) defect is usually found to create shallow acceptor states above the valence band maximum (VBM) and the electronic transition between the conduction band minimum (CBM) and Na_{Zn} acceptors can generate emission peak around 3 to 3.1 eV in the PL spectrum of the Na-doped ZnO thin films.[30,31] Therefore, the UV emission of the $Zn_{0.94}Na_{0.06}O$ films becomes broad and red shifted due to the convergence of the electronic transitions from CBM to both shallow Na_{Zn} acceptor states and to the valence band (band to band transition). Besides shallow acceptor states, the group I alkali elements are also found to create a deep acceptor state with binding energy of ~600−800 meV, which can provide yellow-orange luminescence around 2.2 eV (peak 3) in the PL spectra.[33,34] Therefore, here, in case of $Zn_{0.94}Na_{0.06}O$ films, the observed emission (peak 3) at yellow-orange zone (2.18 eV) can be assigned to the electronic transition from CBM to the deep Na_{Zn} acceptor levels.[33,34] Because of the appearance of yellow-orange emission in the Na-doped ZnO films the defect related band becomes broad and seems to be red-shifted compared with that of the pure ZnO film. Again with the increase of PO_2 from 1×10^{-4} to 1×10^{-3} Torr, the defect-emission band of Na-doped ZnO initially red-shifted due to relative increase of yellow-orange emission intensity. However, for further increase of PO_2 (1×10^{-3} to 1×10^{-2} Torr), the defect-emission band becomes blue-shifted because of dominance of green emission. The entire PL emission processes are described in Figure 7b with a schematic energy band diagram with different defect levels within the ZnO band gap.

It is interesting to notice that all the $Zn_{0.94}Na_{0.06}O$ films are found to exhibit significant green emission centred around 2.38 eV (peak 2), which is found to be enhanced due to Na-doping (Figure 7a). However, the origin of the green emission in ZnO thin films and nanostructures remains quite controversial.[35] Previously, it was suggested that that stabilization of V_O is responsible for green emission in ZnO but, recent studies have shown that it is Zn vacancy also or rather than V_O, which is responsible for green luminescence in ZnO thin films and nanostructures.[12,20,23,35−37] The V_{Zn} defect is found to create deep acceptor level at ~0.9 eV above the VBM and the electronic transition from the CBM to V_{Zn} acceptor levels often leads to the emission of visible green luminescence at 2.35−2.45 eV.[35−37] Here, the $Zn_{0.94}Na_{0.06}O$ film prepared under $P_{O_2} \approx 1 \times 10^{-2}$ Torr exhibits highest green-emission and the intensity of green-emission is found to fall gradually with decrease of P_{O_2}. The V_O concentration is generally known to be inversely proportional to the oxygen partial pressure (P_{O_2}).[23] Therefore, in case of Na-doped ZnO films, the decrease of green emission intensity (I_G) with the decrease of P_{O_2} clearly excludes the possibility of V_O as the origin of green emission. On the other hand, the formation of Zn vacancy (V_{Zn}) in ZnO is found to be energetically favorable under high level of P_{O_2}.[23] Recently, Yi et al.[12] have suggested that the formation energy of V_{Zn} in ZnO can be reduced significantly in presence of the

dx.doi.org/10.1021/am302649r | ACS Appl. Mater. Interfaces 2013, 5, 2455−2461

substitutional Li (Li_{Zn}) and interstitial Li (Li_i) defects through the formation of defect complexes such as V_{Zn} + Li_{Zn} + Li_i and V_{Zn}+ Li_i. Hence, it is quite possible to stabilize considerable amount of V_{Zn} defects through the cationic substitution of alkali metal such as Li, K in ZnO.[12,20] Therefore, similar to the Li and K, in present study, the Na-doping also might favor to stabilize V_{Zn} defects along with the Na substitutional (Na_{Zn}) defects in $Zn_{0.94}Na_{0.06}O$ films, where with the increase of P_{O_2}, the concentration of V_{Zn} increases (evident from PL spectra).The intensity of the green luminescence is also found to decrease gradually with the increase of film-thickness, which indicates that the stabilization of V_{Zn} defects in $Zn_{0.94}Na_{0.06}O$ film might be favored by decreasing the film-thickness. This may be due to the reason that V_{Zn} always prefer to reside at the surface because of low formation energy[18] and therefore, the probability of formation of V_{Zn} defects in a low thickness ZnO film may be high compared to a thicker film.

Therefore, the origin of magnetic moment in Na-doped ZnO films can be attributed mainly to V_{Zn} defects.[12−14] Panels a and b in Figure 8 provide the direct correlation between the M_S and

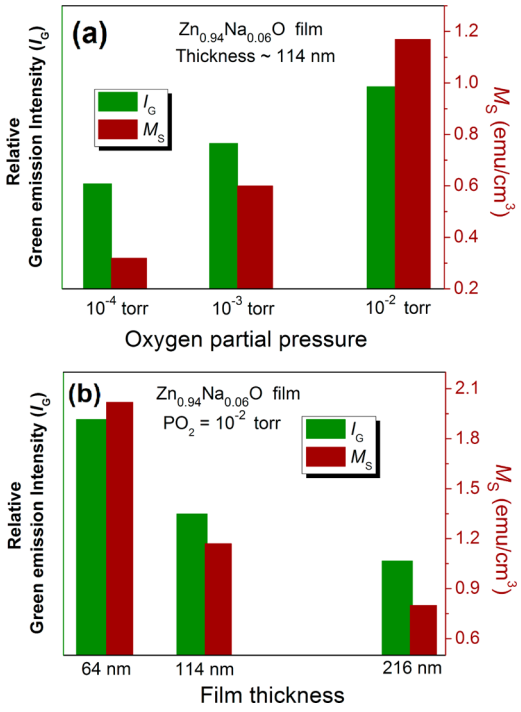

Figure 8. Correlation between the magnitude of M_S and green luminescence intensity (I_G), obtained from PL spectra, in $Zn_{0.94}Na_{0.06}O$ films with various (a) film thickness and (b) P_{O_2}.

green emission intensity (I_G) with the corresponding film-thickness and P_{O_2} respectively. The largest M_S in 64 nm thick $Zn_{0.94}Na_{0.06}O$ film is due to the presence of highest amount of V_{Zn} defects. The variation of M_S is found to follow a similar trend with variation of V_{Zn} concentration. Hence, the observed RTFM in $Zn_{0.94}Na_{0.06}O$ film might be arises due to V_{Zn} defects which stabilize because of Na-doping. Besides V_{Zn} defects, the substitution of Na at Zn site (Na_{Zn}) can also create one hole per alkali atom in the neighbouring oxygen atom.[12,21] The increase of M_S and T_C with the increase of hole concentration (see the inset of Figure 4b) indicates the ferromagnetic interaction between the magnetic moments is mediated by the holes originated due to both Na_{Zn} and V_{Zn} acceptors. The increase of magnetic moment in thinner films can be explained by considering that the V_{Zn} lies on or near to the surface possess larger magnetic moment compared to the V_{Zn} lies deep inside the bulk.[18] The majority of V_{Zn} defects in the thinner $Zn_{0.94}Na_{0.06}O$ films should lie on the surface or near to the surface layer to show large magnetic moment, whereas for thick films most of the V_{Zn} defects lie deep inside, far from the surface and therefore, the overall magnetic moment get reduced. Besides V_{Zn} defect, the Na_{Zn} defects at divalent Zn site can also induce local magnetic moment (~1 μ_B) in ZnO.[12,19,38] Although, the magnetic moment arises due to substitutional Na (Na_{Zn}) defect is comparatively less in magnitude than the V_{Zn} (~2 μ_B) defect, but still would contribute to the overall ferromagnetic moment. Hence, the magnetic moments of both V_{Zn} and Na_{Zn} defects or even their various defect complexes of V_{Zn} and Na_{Zn} defects could be mediated by holes due to Na-doping to stabilize long-range ferromagnetic ordering in p-type Na-doped ZnO films. Pure ZnO film with 69 nm thick showed weak FM due to presence of small amount of V_{Zn} defects. However, similar to case of Na-doped ZnO films, the concentration of V_{Zn} in pure ZnO films also decreases as the thickness of the film increases. As a result the thicker pure ZnO film (~196 nm) does not exhibit RTFM possibly because of a lack of enough V_{Zn} concentration (may be below the required threshold V_{Zn} concentration) to sustain long range ferromagnetic ordering.

4. CONCLUDING REMARKS

In summary, the influence of film thickness and the oxygen pressure (P_{O_2}) on the RT ferromagnetic behaviour of p-type $Zn_{0.94}Na_{0.06}O$ films fabricated by PLD technique are investigated. At a fixed P_{O_2}, the $Zn_{0.94}Na_{0.06}O$ film with lowest thickness (~64 nm) exhibits largest M_S and also highest T_C. On the other hand, the M_S of almost similar thick $Zn_{0.94}Na_{0.06}O$ films is found to decease consistently with decrease of PO_2. The suppression of FM in $Zn_{0.94}Na_{0.06}O$ film with the decrease of P_{O_2} excludes the possibility of oxygen vacancy defects as the origin of RTFM. The substitution of Na^{1+} at Zn site within the ZnO matrix is confirmed by XPS study, whereas the PL spectroscopic measurements have shown the presence of large amount V_{Zn} defects, responsible for the origin of RTFM in $Zn_{0.94}Na_{0.06}O$ films. The V_{Zn} concentration is also found to vary significantly with the film- thickness and PO_2 and so the ferromagnetic response of $Zn_{0.94}Na_{0.06}O$ films. The magnetic contribution from Na_{Zn} defects can also not be discarded because Na_{Zn} can also induce localised magnetic moment. Therefore, the substitution of monovalent Na is found to be effective in stabilizing cation-defect-induced RTFM in ZnO films which can be an alternative approach of preparing new class of ZnO-based high T_C magnetic semiconductor. Our study also demonstrates that the stabilization of such cation-defects-induced RTFM in Na-doped ZnO films is most favorable in the film with relatively low thickness (<70 nm) and prepared under high level of P_{O_2} (>1 × 10^{-2} Torr).

AUTHOR INFORMATION

Corresponding Author

*Phone: +91 (033) 2335 5706-8. Fax: +91 (033) 2335 3477. E-mail: shyam@bose.res.in; sghoshphysics@gmail.com (S.G.).

Present Address

[†]G.G.K is currently at Center for Research in Nanoscience and Nanotechnology, University of Calcutta, Technology Campus, Block JD2, Sector III, Salt Lake City, Kolkata 700 098, India

Notes

The authors declare no competing financial interest.

■ ACKNOWLEDGMENTS

The above work is supported by the CSIR (INDIA) funded project 03(1178)/10/EMR-II. S.G. acknowledges the financial support of Council of Scientific and Industrial Research (CSIR), Government of India, for providing a research fellowship. G.G.K. is thankful to Department of Science and Technology (DST), Government of India, for providing research support through 'INSPIRE Faculty Award' (IFA12-ENG-09). We acknowledge the help of Mr. S. K. Choudhury for XPS experiments at IOP, Bhubaneswar, India.

■ REFERENCES

(1) Zunger, A.; Lany, S. *Physics* **2010**, *3*, 53.
(2) Ghosh, S.; Munshi, D De.; Mandal, K. *J. Appl. Phys.* **2010**, *107*, 123919.
(3) Prinz, G. A. *Science* **1998**, *282*, 1660.
(4) Ohno, H. *Science* **1998**, *281*, 951.
(5) Venkatesan, M.; Fitzgerald, C. B.; Coey, J. M. D. *Nature* **2004**, *430*, 630.
(6) Sundaresan, A.; Bhargavi, R.; Rangarajan, N.; Siddesh, U.; Rao, C. N. R. *Phys. Rev. B* **2006**, *74*, 161306.
(7) Hong, N. H.; Sakai, J.; Poirot, N.; Brizé, V. *Phys. Rev. B* **2006**, *73*, 132404.
(8) Khan, G. G.; Ghosh, S.; Mandal, K. *J. Solid State Chem.* **2012**, *186*, 278.
(9) Xing, G. Z.; Lu, Y. H.; Tian, Y. F.; Yi, J. B.; Lim, C. C.; Li, Y. F.; Li, G. P.; Wang, D. D.; Yao, B.; Ding, J.; Feng, Y. P.; Wu, T. *AIP Advances* **2011**, *1*, 022152.
(10) Ghosh, S.; Khan, G. G.; Mandal, K. *ACS Appl. Mater. Interfaces* **2012**, *4*, 2048.
(11) Gao, F.; Hua, J.; Wang, J.; Yang, C.; Qin, H. *Chemical Physics Letters* **2010**, *57*, 488.
(12) Yi, J. B.; Lim, C. C.; Xing, G. Z.; Fan, H. M.; Van, L. H.; Huang, S. L.; Yang, K. S.; Huang, X. L.; Qin, X. B.; Wang, B. Y.; Wu, T.; Wang, L.; Zhang, H. T.; Gao, X. Y.; Liu, T.; Wee, A. T. S.; Feng, Y. P.; Ding, J. *Phys. Rev. Lett.* **2010**, *104*, 137201.
(13) Li, Y.; Deng, R.; Yao, B.; Xing, G.; Wang, D.; Wu, T. *Appl. Phys. Lett.* **2010**, *97*, 102506.
(14) Xu, X. G.; Yang, H. L.; Wu, Y.; Zhang, D. L.; Wu, S. Z.; Miao, J.; Jiang, Y.; Qin, X. B.; Cao, X. Z.; Wang, B. Y. *Appl. Phys. Lett.* **2010**, *97*, 232502.
(15) Pemmaraju, C. D.; Sanvito, S. *Phys. Rev. Lett.* **2005**, *94*, 217205.
(16) Elfimov, I. S.; Yunoki, S.; Sawatzky, G. A. *Phys. Rev. Lett.* **2002**, *89*, 216403.
(17) Rahman, G.; García-Suárez, V. M.; Hong, S. C. *Phys. Rev. B.* **2008**, *78*, 184404.
(18) Wang, Q.; Sun, Q.; Chen, G.; Kawazoe, Y.; Jena, P. *Phys Rev. B* **2008**, *77*, 205411.
(19) Bouzerar, G.; Ziman, T. *Phys. Rev. Lett.* **2006**, *96*, 207602.
(20) Ghosh, S.; Khan, G. G.; Das, B.; Mandal, K. *J. Appl. Phys.* **2011**, *109*, 123927.
(21) Ghosh, S.; Khan, G. G.; Varma, S.; Mandal, K. *J. Appl. Phys.* **2012**, *112*, 043910.
(22) Gu, H.; Jiang, Y.; Xu, Y.; Yan, M. *Appl. Phys. Lett.* **2011**, *98*, 012502.
(23) Børseth, T. M.; Svensson, B. G.; Kuznetsov, A. Yu.; Klason, P.; Zhao, Q. X.; Willander, M. *Appl. Phys. Lett.* **2006**, *89*, 262112.
(24) Wagner, C. D.; Riggs, W. M.; Davis, L. E.; Moulder, J. F.; Muilenberg, G. E. *Handbook of X-ray Photoelectron Spectroscopy*; Perkin Elmer: Eden Prairie, MN, 1979.
(25) Mishra, D. K.; Kumar, P.; Sharma, M. K.; Das, J.; Singh, S. K.; Roul, B. K.; Varma, S.; Chatterjee, R.; Srinivasu, V. V.; Kanjilal, D. *Physica B* **2010**, *405*, 2659.
(26) Gu, Z. B.; Lu, M. H.; Wang, J.; Wu, D.; Zhang, S. T.; Meng, X. K.; Zhu, Y. Y.; Zhu, S. N.; Chena, Y. F. *Appl. Phys. Lett.* **2006**, *88*, 082111.
(27) Joshi, A. G.; Sahai, S.; Gandhi, N.; Radha Krishna, Y. G.; Haranatha, D. *Appl. Phys. Lett.* **2010**, *96*, 123102.
(28) Lv, J.; Huang, K.; Chen, X.; Zhu, J.; Cao, C.; Song, X.; Sun, Z. *Opt. Commun.* **2011**, *284*, 2905.
(29) Lin, S. S.; He, H. P.; Lu, Y. F.; Yeb, Z. Z. *J. Appl. Phys.* **2009**, *106*, 093508.
(30) Park, C. H.; Zhang, S. B.; Wei, S. H *Phys. Rev. B* **2002**, *66*, 073202.
(31) Lee, E. C.; Chang, K. J. *Phys. Rev. B* **2004**, *70*, 115210.
(32) Kong, Y. C.; Yu, D. P.; Zhang, B.; Fang, W.; Feng, S. Q. *Appl. Phys. Lett.* **2001**, *78*, 407.
(33) Rauch, C.; Gehlhoff, W.; Wagner, M, R.; Malguth, E.; Callsen, G.; Kirste, R.; Salameh, B.; Hoffmann, A.; Polarz, S.; Aksu, Y.; Driess, M. *J. Appl. Phys.* **2010**, *107*, 024311.
(34) Meyer, B. K.; Stehr, J.; Hofstaetter, A.; Volbers, N.; Zeuner, A.; Sann, J. *Appl. Phys. A* **2007**, *88*, 119.
(35) Janotti, A.; Van de Walle, C. G. *Phys. Rev. B* **2007**, *76*, 165202.
(36) Reynolds, D. C.; Look, D. C.; Jogai, B.; Morkoc, H. *Solid State Commun.* **1997**, *101*, 643.
(37) Reynolds, D. C.; Look, D. C.; Jogai, B.; Van Nostrand, J. E.; Jones, R.; Jenny, J. *Solid State Commun.* **1998**, *106*, 701.
(38) Dev, P.; Zhang, P. *Phys. Rev. B* **2010**, *81*, 085207.